Naphthalene-containing polyamines supported in nanosized boehmite particles†

Ricardo Aucejo,[a] Pilar Díaz,[a] Enrique García-España,*[a] Javier Alarcón,*[b] Estefanía Delgado-Pinar,[b] Francisco Torres,[b] Conxa Soriano[c] and M. Carmen Guillem[d]

Received (in Durham, UK) 20th June 2006, Accepted 29th September 2006
First published as an Advance Article on the web 30th October 2006
DOI: 10.1039/b608678k

Boehmite nanoparticles with covalently linked polyamine chains functionalized with naphthalene fluorophores have been prepared and characterized. The characterization of the materials by elemental microanalysis, X-ray powder diffraction, MAS ^{29}Si NMR and electron microscopy unambiguously prove that the covalent anchorage had occurred. Steady-state fluorescence emission studies show that the luminescent properties of the modified nanoparticles are sensitive to changes in concentration of hydrogen ions, metal ions and anionic nucleotides such as ATP. The behaviour of the attached materials in aqueous solution is parallel to the behaviour of the single fluorophoric polyamines. Comparisons are established with analogous systems containing indole as a fluorophore.

Introduction

In recent years the functionalization of nanoparticles with organic components for a variety of goals has received much interest.[1] However, most of these particles were silica or gold-based and as far as we know there were no studies performed on boehmite-based particles. In this regard, we have recently reported on new sensing systems based on nano-sized boehmite as support of indole-containing polyamines.[2] Steady-state fluorescence emission studies showed that these materials presented a very efficient sensing ability for hydrogen ions, metal cations and anionic nucleotides.

Boehmite nanoparticles used as a support present some characteristic features that render the material very useful. First, it was possible to carry out the measurements in pure water due to the formation of a colloidal solution that did not perturb the collection of the data. Second, the nanoparticles could be easily recovered after their use by filtration because a change from a sol to a gel state occurs on increasing the pH. Third, the prepared boehmite particles, which were in the 20–40 nm range, have a very high specific surface increasing the probability for anchoring organic components. Fourth, the terminal hydroxyl groups at the boehmite surface provide a high hydrophilic character improving the surface reactivity.[3,4]

In view of the behaviour of the materials it seemed interesting to check the possibility of anchoring other fluorophores. In this paper we have used naphthalene as a fluorophoric unit. The main reason for our choice resided on the well-known photochemical behaviour of naphthalene and on its photochemical and thermal stability. Moreover, in previous works[5,6] we had examined the photochemical behaviour of the naphthalene polyamine molecules in water and therefore could make direct comparisons with the polyamines when supported on the boehmite surface. This last characteristic is very important because it would permit prediction of the characteristics of the supported systems by just analysing the behaviour of the non-supported molecules.

With this purpose, we have prepared three new organic–inorganic covalently linked materials which contain naphthalene as fluorophore, the polyamine as coordination site and boehmite as a support. The materials will be named as B1NNp, B2NNp and B3NNp where B stands for boehmite, 1N, 2N and 3N for the number of nitrogen atoms in the polyamine chain and Np for naphthalene. We have examined the photochemical response of the supported materials in aqueous solution at variable pH and with respect to Cu^{2+}, Zn^{2+}, Cd^{2+} and Pb^{2+} coordination. For comparison, we have studied the behaviour of the non-supported receptor 3NNp (see Scheme 1).

Experimental section

(3-Aminopropyl)triethoxysilane (98%), *N*-[3-(trimethoxysilyl)propyl]ethylenediamine (97%), *N*′-[3-(trimethoxysilyl)propyl]diethylenetriamine (technical grade) and naphthalene-1-carboxaldehyde were commercially available Aldrich reagents and were used without further purification. Adenosine 5′-triphosphate (ATP), adenosine 5′-diphosphate (ADP) and adenosine 5′-monophosphate (AMP) were 98% purity

[a] *Departament de Química Inorgànica, ICMOL, Facultat de Química, Universitat de València, Burjassot, Spain. E-mail: enrique.garcia-es@uv.es; Fax: 963544322; Tel: 963544879*
[b] *Departament de Química Inorgànica, Facultat de Química, Universitat de València, Burjassot, Spain. E-mail: javier.alarcon@uv.es; Fax: 963544322; Tel: 963544584*
[c] *Departament de Química Orgánica, ICMOL, Facultat Farmacia, Universitat de València, Burjassot, Spain*
[d] *Departament de Química Inorgànica, ICMUV, Facultat de Química, Universitat de València, Burjassot, Spain*
† Electronic supplementary information (ESI) available: Fig. S1–S11 and Table S1. See DOI: 10.1039/b608678k

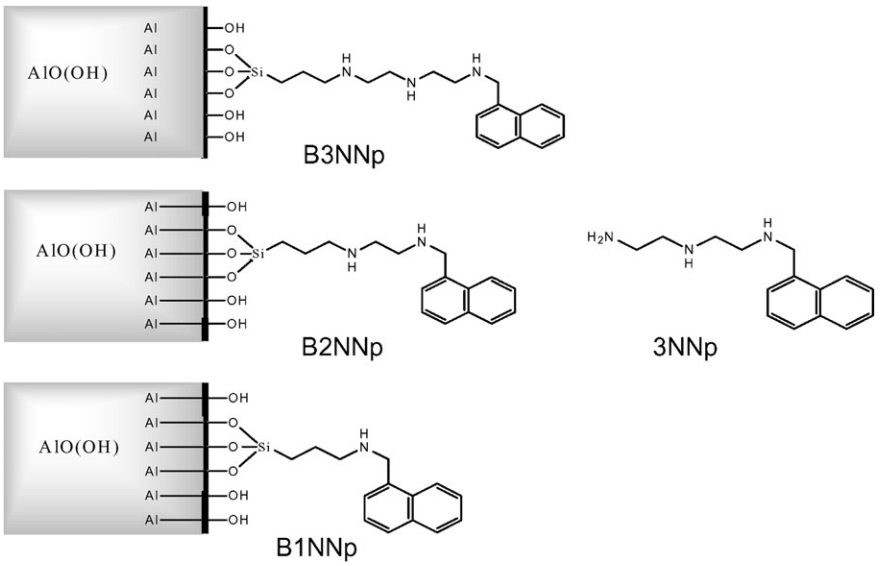

Scheme 1

reagents purchased from Aldrich. AlO^{s}Bu and nitric acid used in the synthesis of the boehmite particles were obtained from Aldrich. The methanol and ethanol of analytical grade used in the preparation were dried over 4 Å molecular sieves. All the reactions in the synthetic procedure were carried out under a nitrogen atmosphere. All solutions used for the fluorimetric and potentiometric titrations were prepared with ultrapure water.

Preparation of the materials

Boehmite particles were synthesized as previously reported following a two-step procedure (Scheme 2).[2] The first step was the hydrolysis of aluminium s-butoxide in an excess of water at 80 °C under vigorous stirring. After the alkoxide addition, an exothermic reaction took place and a gel was formed almost immediately, which was held under stirring for several hours. The second step, a peptization process, was carried out keeping the boehmite particles in a nitric acid solution at 90 °C for 1 week.

The anchoring of the sensors to the surface of the nanoparticles has been achieved by direct hydrolysis of the OH groups located all around the surface of the boehmite particles, and the hydrolysable alkyl groups bonded to the silicon atom attached to the polyamine molecules.

Boehmite supported B1NNp. 1.65 g (7.5 mmol) of (3-aminopropyl)triethoxysilane were placed in a round-bottom flask and solved in 100 cm^3 of ethanol. Then a solution of 1.2 g (7.65 mmol) of naphthalene-1-carboxaldehyde in 50 cm^3 of ethanol was added dropwise. The resulting mixture was stirred for two hours at rt and then a 4-fold excess of sodium borohydride (1.17 g, 30.6 mmol) was added. The reaction was kept for a further hour under stirring and then 1.5 g of boehmite was added. After 1 day stirring at rt, the obtained white solid was separated by centrifugation.

Then, the solid was repeatedly leached with ethanol, dichloromethane and finally with ether, being collected in every step by centrifugation. Anal.: C 6.35%; N 0.55%; H 2.77%.

Boehmite supported B2NNp. The above method was repeated using 1.2 g (5.3 mmol) of *N*-[3-(trimethoxysilyl)propyl] ethylenediamine, 0.79 g (5.1 mmol) of naphathalene-1-

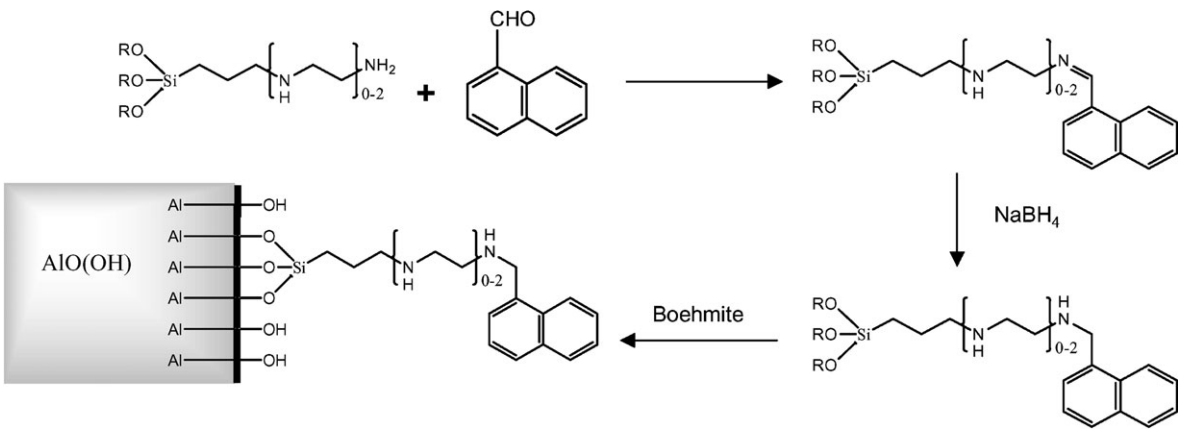

Scheme 2

carboxaldehyde and 1.0 g of boehmite. Anal.: C 8.11%; N 1.09%; H 2.94%.

Boehmite supported B3NNp. The above method was repeated using 1.3 g (5.0 mmol) of *N*-[3-(trimethoxysilyl)propyl]diethylenetriamine, 0.82 g (5.2 mmol) of naphathalene-1-carboxaldehyde and 1.1 g of boehmite. Anal.: C 8.14%; N 1.34%; H 2.95%.

Materials and methods

X-ray diffraction analysis was performed on a Siemens D-5000 difractometer using graphite monochromatic CuK_α radiation (λ = 1.5418 Å). Powdered samples were sprayed on glass sample holders and data collected in Bragg–Brentano geometry from 5 to 65° 2θ with a step-size of 0.02° 2θ and a counting time of 5 s per step.

Infrared transmission spectra were obtained with a Perkin Elmer spectrometer Model 882 in the range 400–1400 cm^{-1} using the KBr pellet method.

The morphology of as-prepared and sensor-containing boehmite particles was examined using a Jeol 1010 transmission electron microscope at an accelerating voltage of 100 kV. Samples were prepared by dispersing as-produced powders in absolute ethanol and setting dropwise on copper grids that had previously been coated with a holey thin carbon film.

^{29}Si NMR studies were carried out on a Varian UNITY 300 spectrometer at a resonance frequency of 59.59 MHz. The MAS NMR spectra were recorded with a 7 mm zirconium oxide rotor spinning at 4.5 kHz. A 90° single-pulse was used with an acquisition time of 0.080 s and a delay time of 60 s. Chemical shifts were measured relative to tetramethylsilane (TMS).

Ultraviolet–visible spectra of the boehmite-supported molecules were recorded on a Shimadzu UV 2101 PC spectrometer. The absorption measurements were performed at room temperature, in the 200–500 nm range, using water as reference.

Fluorescence spectra of grafted molecules were obtained with a PTI MO-5020 spectrofluorimeter. The emission spectra were measured from 300 to 500 nm for a excitation wavelength of 280 nm, corresponding to the maximum of the excitation intensity. Fluorescence quantum yield have been measured referring the values to the previously calculated quantum yield of 3NNp (ϕ_0 = 0.18 in water).[7] The solvent used was water and the pH was kept at 3.0 for the three materials. Solutions of the materials were prepared by suspension of 10 mg of the corresponded material in 10 mL of water. The concentration of the nucleotide solutions were *ca.* 0.1 mol dm^{-3}.

emf Measurements

The potentiometric titrations were carried out at 298.1 ± 0.1 K using NaCl 0.15 mol dm^{-3} as supporting electrolyte. The experimental procedure (burette, potentiometer, cell, stirrer, microcomputer, *etc.*) has been fully described elsewhere.[8] The acquisition of the emf data was performed with the computer program PASAT.[9] The reference electrode was an Ag/AgCl electrode in saturated KCl solution. The glass electrode was calibrated as a hydrogen-ion concentration probe by titration of previously standardized amounts of HCl with CO_2-free NaOH solutions and the equivalent point determined by the Gran′s method,[10] which gives the standard potential, $E^{\circ\prime}$, and the ionic product of water (pK_w = 13.73(1)).

The computer program HYPERQUAD was used to calculate the protonation and stability constants.[11] The pH range investigated was 2.0–11.0 and the concentration of the metal ions and of the ligands ranged from 1×10^{-3} to 5×10^{-3} mol dm^{-3} with M : L molar ratios 1 : 1. The different titration curves for each system (at least two) were treated either as a single set or as separated curves without significant variations in the values of the stability constants. Finally, the sets of data were merged together and treated simultaneously to give the final stability constants. The stability constants for the systems ATP-3NNp, ADP-3NNp and AMP-3NNp were taken from ref. 6. The distribution diagrams were plotted with the HYSS program.[12]

Results and discussion

Preparation and characterization of the materials

The boehmite nanoparticles were prepared and characterized as described in ref. 2. The synthetic approach used to anchor the fluorophores to the boehmite surface was similar to that used in ref. 2 for the preparation of the analogous indole-containing compounds. Basically, it consists of a two-step procedure. In the first step, naphthalene-1-carbaldehyde is reacted with the corresponding precursor tri(alkoxy)polyaminosilane to yield the Schiff bases which are characterized by a downfield shifted ^1H NMR signal at *ca.* 8.4 ppm attributable to the imine-type proton. The imines are reduced with sodium borohydride to give the corresponding functionalized fluorophoric precursors. The controlled hydrolysis of the precursors in the presence of peptized boehmite nanoparticles gave the supported materials. Extensive washing of the materials was successively performed with ethanol, dichloromethane and diethyl ether. The amount of attached polyamines was determined taking into account the C, H, N elemental microanalysis. The number of moles of polyamine attached per gram of boehmite was 2.9×10^{-4}, 3.9×10^{-4} and 3.2×10^{-4} for B1NNp, B2NNp and B3NNp, respectively. Although these numbers are not very large, they are enough to have a large emissive response upon interaction with the different substrates (*vide infra*).

The final supported materials were checked by conventional solid state techniques. X-Ray powder diffractograms of B1NNp, B2NNp and B3NNp (Fig. 1) present peaks at 13.7°, 28.3°, 38.4°, 49.2° and 64.8° 2θ which are characteristic of the boehmite structure and confirms that the matrix has not been disrupted throughout the synthetic procedure.

This observation is also supported by the infrared spectra of the three final materials (Supplementary material†).

Transmission electron microscopy of the samples reveals that the boehmite particles are dispersed. The mean size of the particles (20 nm, Fig. 2) is smaller than that previously obtained for the boehmite indole materials.[2] Curiously, in these new materials the shape of the functionalized particles

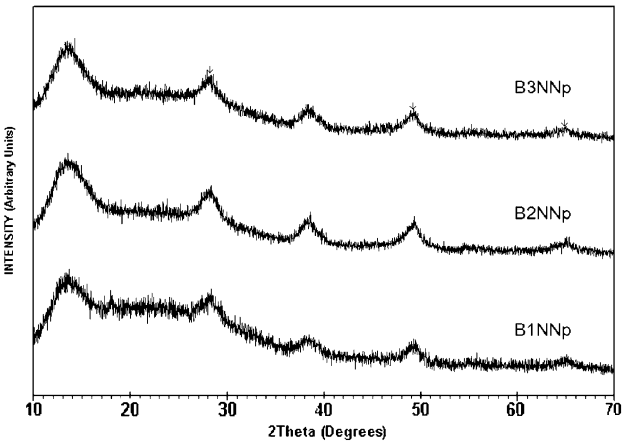

Fig. 1 Powder X-ray diffraction patterns for B1NNp, B2NNp and B3NNp.

is much more round than those with indole which presented square cross-sections.

MAS ^{29}Si NMR spectra of the three materials show broad signals at *ca.* −40 and −110 ppm (Fig. 3). The first one can be ascribed to the presence of the so-called T-units (C–$(SiO)_3$) while the second one seems to indicate that part of the material has evolved to give Q-units (SiO_4). Moreover, it has been stated that each substitution of a Si atom by an Al one yields a 5–7 nm upfield shift of the signal which initially should appear at *ca.* 70 ppm. Therefore, in our case the position of the most shielded peak (50 ppm) suggests that three of the silicon atoms

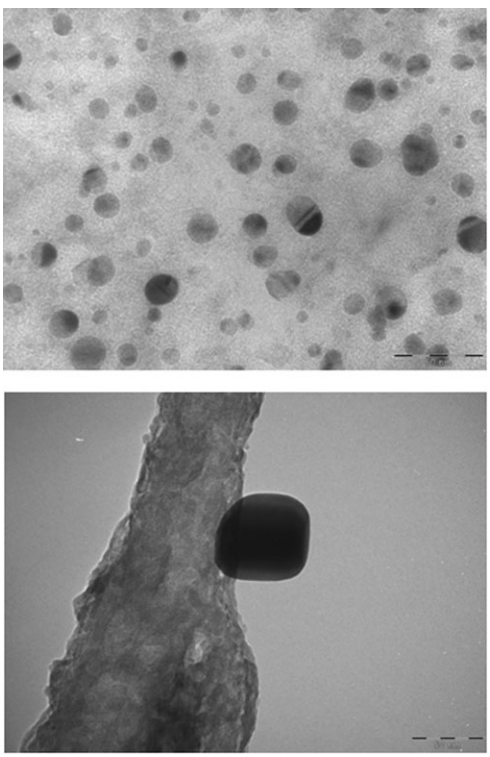

Fig. 2 Top: Micrograph of the boehmite grafted B3NNp material showing the presence of 20 nm dispersed particles (bar = 50 nm). Bottom: Detailed view of a single particle (bar 50 nm).

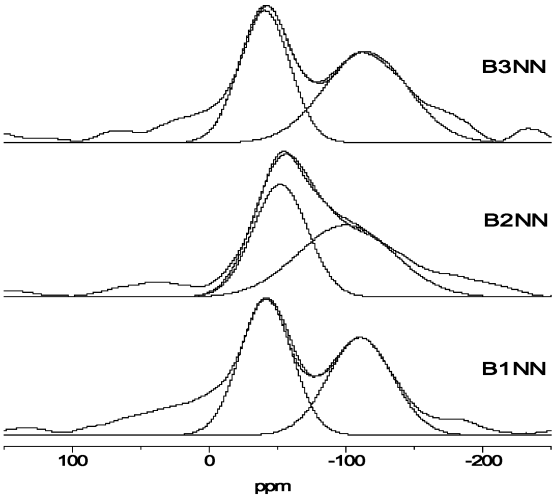

Fig. 3 Experimental and deconvoluted ^{29}Si NMR spectra of B1NIn, B2NIn and B3NIn.

in the CH_2–Si–$(OSi)_3$– are replaced by aluminium. The appearance of Q signals should imply the partial break of the Si–C bonds. This finding has been reported to occur when activating species like phenols are present in the reaction medium.[13,14]

Steady-state fluorescence emission studies

In order to characterise the photochemical properties of these polyamines we have carried out steady-state fluorescence studies on the supported naphthalene containing polyamines and on their interaction with the metal ions Cu^{2+}, Zn^{2+}, Cd^{2+}, Pb^{2+} and Co^{2+} as well as with the nucleotides ATP, ADP and AMP. For comparison with the behaviour of the free polyamines we have taken *N*-{2-[[(naphtalen-1-ylmethyl)amino]ethyl}ethane-1,2-diamine (3NNp) as a reference.[5,6] With this polyamine we completed the complexation studies with Cu^{2+}, Zn^{2+}, Cd^{2+}, Pb^{2+} and Co^{2+} that had not yet been reported. The studies for both the supported and non-supported molecules were conducted in pure water. The colloidal nature of the supported materials at pH below 9 permitted neat spectra not disturbed by light scattering to be obtained.

The fluorescence emission spectra of B3NNp recorded upon excitation at 280 nm shows a band centred at 335 nm whose intensity decreases with the pH (Fig. 4). The fluorescence intensity *vs.* pH curve (Fig. 5 top) displays two clear diminutions in fluorescence when the pH of the colloidal solution is raised from 2 to 12. The first one is produced at a mean pH of 4 while the second one occurs at pH *ca.* 9. Between them the intensity remains practically constant.

The variation of the fluorescence of the free molecule 3NNp shows a similar trend with the decreases in intensity occurring in the same pH range. As shown in Fig. 5 (bottom), such decreases correspond to the first and second deprotonation processes of the polyamine.[5] The plateau region between pH values 4 and 8 corresponds to the predominance in solution of the diprotonated $H_2(2NNp)^{2+}$ species. Comparison between Fig. 5 top and bottom indicates that covalent anchoring to

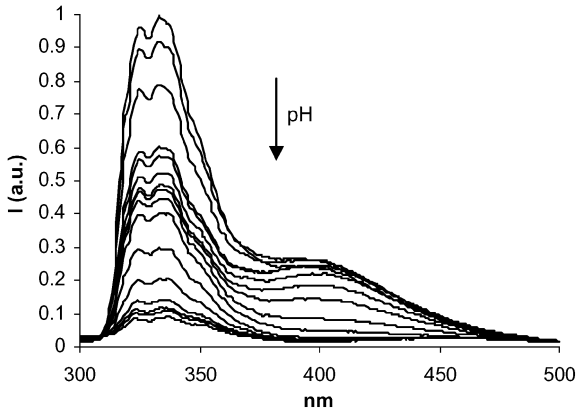

Fig. 4 Steady-state fluorescence emission for B3NNp (λ_{exc} = 280 nm) (pH values: 2.22, 2.97, 3.71, 4.58, 4.97, 5.90, 6.45, 7, 7.58, 7.95, 8.66, 9.21, 9.73, 10.23, 10.99, 11.71).

boehmite does not significantly alter the spectroscopic features of the molecule.

For the other materials the emission intensity *vs.* pH curves have profiles that correspond with the number of amino groups in each one of them (Fig. 6). For instance, B1NNp with only one amino group shows one lowering in intensity at *ca.* pH 9. Although B2NNp displays a sharp decrease in intensity at pH 4 corresponding to its first deprotonation, the second one occurring at pH 9 just produces a weak diminution in fluorescence.

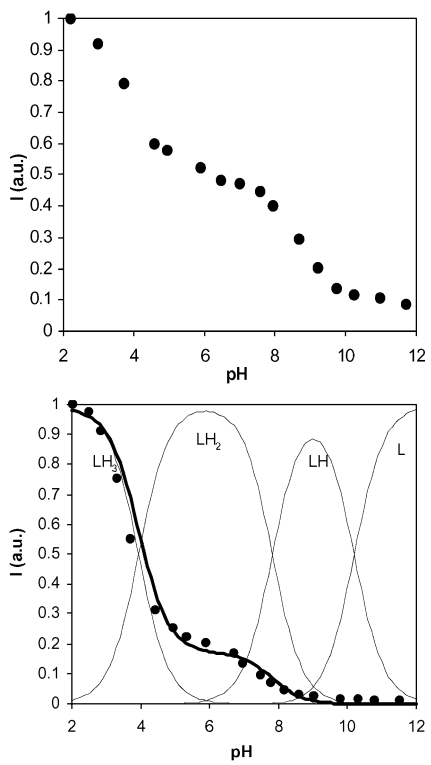

Fig. 5 Fluorescence emission intensity *vs.* pH curves recorded in water for: (Top) B3NNp, (Bottom) 3NNp.

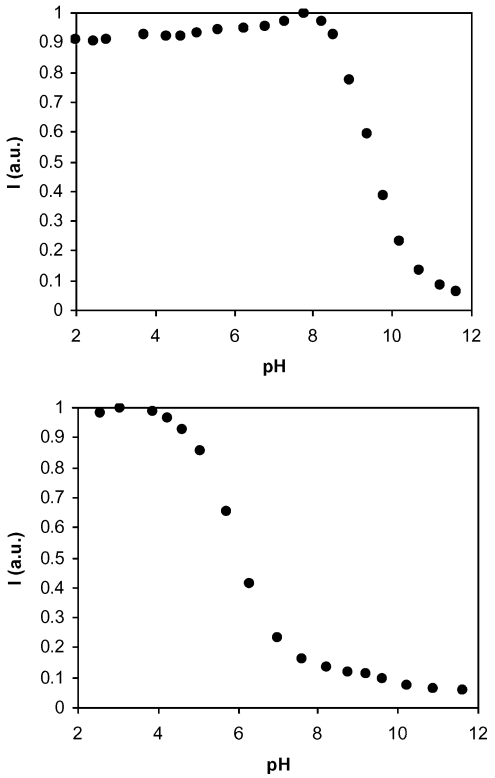

Fig. 6 Fluorescence emission intensity *vs.* pH curves recorded in water for: (Top) B1NNp, (Bottom) B2NNp.

The quantum yields of the three materials have been calculated at pH 3 and are Φ = 0.18, Φ = 0.16 Φ = 0.12 for B1NNP, B2NNp and B3NNP, respectively.

Cu^{2+}, Zn^{2+}, Cd^{2+}, Pb^{2+} and Co^{2+} interaction. First, the variation of the fluorescence with increasing amounts of Cu^{2+} and Zn^{2+} was checked for the three materials at pH values high enough to permit full formation of the complex species (pH 6 and 9 for Cu^{2+} and Zn^{2+}, respectively) (see Supplementary Material†). However, in the case of B1NNp addition of anyone of these metal ions produced just precipitation of the corresponding hydroxides due to the low binding ability of this material containing just one amino group in the lateral chains.

Addition of Cu^{2+} solutions to the other two materials produces a quenching of the emission intensity (CHEQ effect).[15,16] While for B2NNp a 10-fold excess of Cu^{2+} is required to reach the maximum effect, for B3NNp the maximum quenching is already achieved with an equimolar amount of the metal ion. In the case of Zn^{2+} addition, the effect is opposite leading to an enhancement of the fluorescence emission (CHEF effect). Again, for achieving a maximum of the enhancement B3NNp needs less excess of Zn^{2+} than B2NNp. While Zn^{2+} coordination blocks to some extent the electron pairs of the nitrogen atoms partly preventing the photoinduced electron transfer from the amino groups to the excited fluorophore, coordination of Cu^{2+} provides means for the non-radiative deactivation of the emissive state switching off the fluorescence.[17]

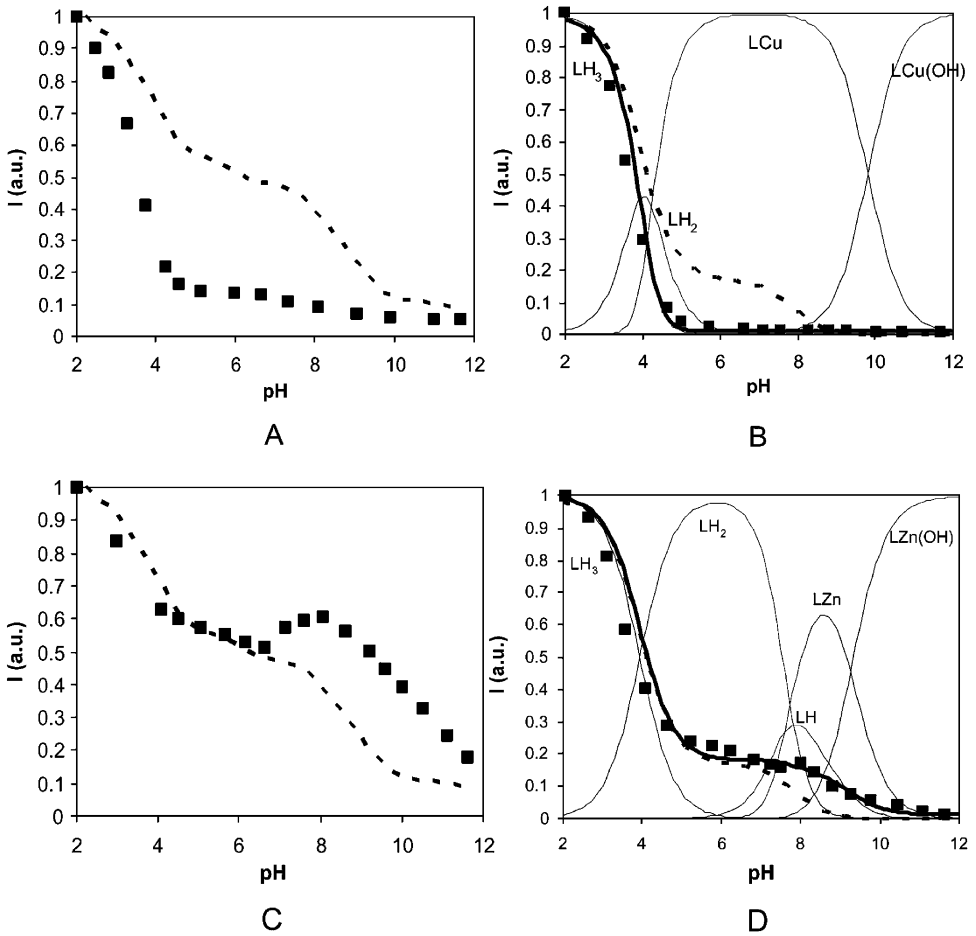

Fig. 7 Fluorescence emission intensity *vs.* pH curves recorded in water for the systems: (A) B3NNp + Cu^{2+}, (B) 3NNp + Cu^{2+}, (C) B3NNp + Zn^{2+}, (D) 3NNp + Zn^{2+}.

Fig. 7 collects the variations of the fluorescence with pH for the systems Cu^{2+}–B3NNp and Zn^{2+}–B3NNp in molar ratio 1 : 1 compared with the emission of the materials in the absence of metal ions (dotted lines). In the same figure are included for comparison analogous studies for the non-supported 3NNp polyamine. The amount of polyamine attached to the boehmite surface has been calculated from the elemental microanalysis.

Fig. 7A shows that the CHEQ effect produced by addition of Cu^{2+} begins at very acidic pH leading to a sharp and almost complete switch off of the fluorescence at pH 4 (basal fluorescence is *ca.* 10%). Comparison with the non-supported polyamines (Fig. 7B) indicates that although the pH range at which the quenching occurs is almost the same for the supported and non-supported polyamines, the effect is much more pronounced when the polyamine is attached to the boehmite nanoparticles. Fig. 7B displays the distribution diagram calculated using the stability constants for the system Cu^{2+}–3NNp determined by potentiometry at 298.1 K in 0.15 mol dm^{-3} NaCl and the changes in fluorescence with pH for 3NNp and for Cu^{2+}–3NNp. Inspection of this figure indicates that the quenching starts with the formation of the $Cu(3NNp)^{2+}$ species ($\log K_{CuL/Cu \cdot L}$ = 14.79(1)) which occurs below pH = 4.

For the system Zn^{2+}–B3NNp the CHEF initiates at pH 7, increasing until it reaches a maximum at pH 9 and then decreases for higher pH values (Fig. 7C). Comparison with non-supported 3NNp reveals that a small CHEF is produced by the formation of the $Zn(3NNp)^{2+}$ species ($\log K_{ZnL/Zn \cdot L}$ = 7.75(2)) (Fig. 7D). The subsequent diminution in fluorescence can be attributed to formation of the hydroxylated $[Zn(3NNp)(OH)]^{2+}$ species ($\log K_{ZnL(OH)/Zn \cdot L}$ = −1.51(3)).[17,18] As happened for Cu^{2+}, the effect is much more remarkable when the polyamine is linked to the boehmite surface. Analogous CHEFF effects are observed for supported B3NNp and free 3NNp in the presence of Cd^{2+} and Pb^{2+} ions (see Supporting Material†). However, the observed effect is less pronounced due to the smaller charge to size ratio of these metal ions that will thereby exert less protective effect.[1,17] In contrast, above pH 7.5 Co^{2+} produces, in correspondence with the formation of the Co^{2+} complexes, a CHEQ effect both in the supported material and in the free molecule (see Supporting Information†).

Interaction with ATP

In order to check the effect of nucleotidic anions on the supported systems we have studied their interaction with

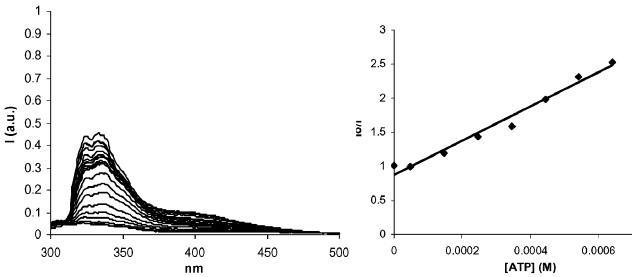

Fig. 8 Left: Variation with pH of the emission spectra of the system B3NNp + ATP. Right: Stern–Volmer plot of the system B3NNp + ATP at pH = 3.

ATP. Fig. 8 plots the variation in the emission of a colloidal solution of B3NNp at pH = 3.0 when increasing amounts of ATP are added. The corresponding plots for B2NNp and B1NNp are included in the supplementary materials.

Stern–Volmer plots for the system ATP–B3NNp fit to a straight line from which a stability constant of 3.4 logarithmic units can be derived for the static quenching at this pH.

Fig. 9 plots the variation of fluorescence emission with pH for the three supported molecules in the presence of a 3-fold excess of ATP. As can be seen in the figure, the quenching effect of ATP is maintained over all the pH range under study. This makes a clear difference with the solution behaviour. For instance, as shown in Fig. 10 for the system ATP–3NNp in mole ratio 10 : 1, ATP only quenches the emission of the non-supported 3NNp at pH values lower 5 in correspondence with the formation of the H_5AL^+ species (A = ATP, L = 2NNP). In such species the adenine ring is protonated becoming more

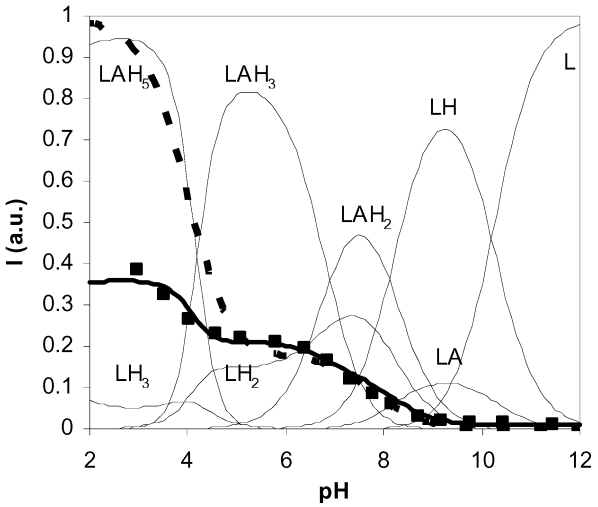

Fig. 10 Fluorescence emission intensity *vs.* pH curves recorded in water for the systems: 3NNp + ATP.

electron-deficient and a photoinduced electron transfer from the excited fluorophore occurs. The constants for the interaction of ATP with the non-supported 3NNp have been calculated by means of pH-metric measurements carried out at 298.1 K in 0.15 mol dm^{-3} NaCl. The results are shown in the Table 1 and denote that the interaction becomes higher as the protonation degree of the polyamine increases.

At acidic pH where adenine is protonated the interaction decreases again due to the reduction of the negative charge of the guest. In the supported materials the constants obtained at pH = 3 are almost equal for the three supported polyamines

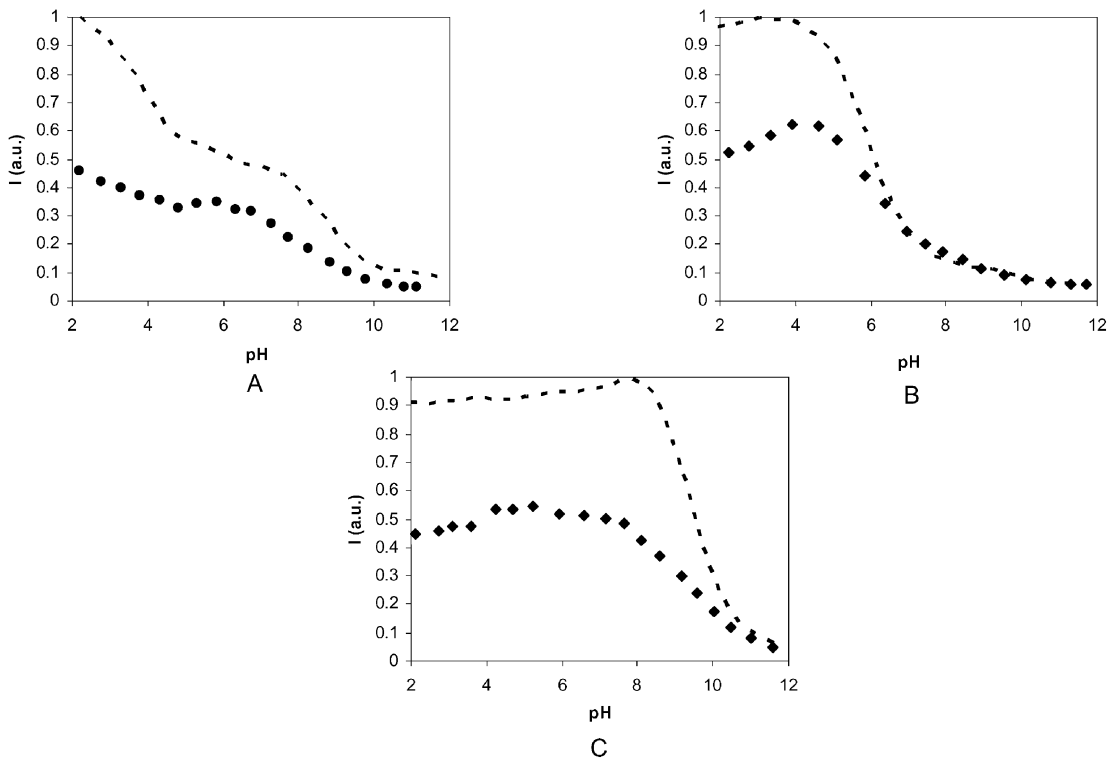

Fig. 9 Fluorescence emission intensity *vs.* pH curves recorded in water for the systems: (A) B3NNp + ATP, (B) B2NNp + ATP, (C)B1NNp + ATP.

Table 1 Stability constants for the interaction of ATP with 3NNp determined at 298.1 K in 0.15 M NaCl

Reaction	log*K*
$3NNp + ATP^{4-} + H^{+} = [H(3NNp)(ATP)]^{3-}$	13.39(2)[a]
$3NNp + ATP^{4-} + 2H^{+} = [H_2(3NNp)(ATP)]^{2-}$	22.33(2)
$3NNp + ATP^{4-} + 3H^{+} = [H_3(3NNp)(ATP)]^{-}$	29.23(2)
$3NNp + ATP^{4-} + 4H^{+} = [H_4(3NNp)(ATP)]$	34.05(3)
$3NNp + ATP^{4-} + 5H^{+} = [H_5(3NNp)(ATP)]^{+}$	37.60(3)
$[H(3NNp)]^{+} + ATP^{4-} = [H(3NNp)(ATP)]^{3-}$	3.59
$[H_2(3NNp)]^{2+} + ATP^{4-} = [H_2(3NNp)(ATP)]^{2-}$	4.29
$[H_2(3NNp)]^{2+} + HATP^{3-} = [H_3(3NNp)(ATP)]^{-}$	4.52
$[H_3(3NNp)]^{3+} + HATP^{4-} = [H_4(3NNp)(ATP)]^{-}$	5.40
$[H_2(3NNp)]^{2+} + H_2ATP^{2-} = [H_4(3NNp)(ATP)]$	5.23
$[H_3(3NNp)]^{3+} + H_2ATP^{2-} = [H_5(3NNp)(ATP)]^{+}$	4.85

(B1NNp, log*K* = 3.5; B2NNp, log*K* = 3.4; B3NNp, log*K* = 3.4) which can be explained taking into account that the dinucleotides is already diprotonated at this pH. On the other hand, the maintenance of the quenching in the supported polyamines throughout the entire pH range suggests that an amplification of the stacking can occur.

Conclusions

We have extended the chemosensing systems based on nano-sized boehmite particles and chromophore-containing polyamines to naphthalene. The synthetic procedure is similar to that previously described for indole-containing nanoparticles providing a simple way to obtain the final materials. The key is the sol–gel anchoring of the tris(alkoxy)polyamino precursor to the boehmite surface. The photochemical behaviour of the supported materials keeps in many instances a reasonable parallelism with the solution behaviour and confirms the potentiality of these materials for building up chemosensing devices.

Acknowledgements

Financial support from DGICYT project BQU2003-09215-CO1 (Spain) is gratefully acknowledged. P. D. thanks MCYT of Spain for Juan de la Cierva contract. R.A. thanks MCYT for a FPU grant.

References

1 (*a*) H. Ow, D. R. Larson, M. Srivastava, B. A. Baird, W. W. Webb and U. Wiesner, *Nano Lett.*, 2005, **5**, 113–117; (*b*) M. Montalti, L. Prodi and N. Zaccheroni, *J. Mater. Chem.*, 2005, **15**, 2810–2814; (*c*) A. B. Descalzo, M. D. Marcos, R. Martínez-Máñez, J. Soto, D. Beltrán and P. Amorós, *J. Mater. Chem.*, 2005, **15**, 2721–2731; (*d*) M. Campàs and I. Katakis, *Anal. Chim. Acta*, 2006, **556**, 306–312; (*e*) B. Gautier and M. Smaïhi, *New J. Chem.*, 2004, **28**, 457–461; (*f*) T. Welzel, I. Radtke, W. Meyer-Zaika, R. Heumann and M. Epple, *J. Mater. Chem.*, 2004, **14**, 2213–2217; (*g*) M. Montalti, L. Prodi, N. Zaccheroni, A. Zattoni, P. Reschiglian and G. Falini, *Langmuir*, 2004, **20**, 2989–2991; (*h*) K. G. Thomas and P. V. Kamat, *Acc. Chem. Res.*, 2003, **36**, 888–898; (*i*) G. Zhang, A. Niu, S. Peng, M. Jiang, Y. Tu, M. Li and C. Wu, *Acc. Chem. Res.*, 2001, **34**, 249–256; (*j*) M. N. V. Ravi Kumar, *J. Pharm. Pharm. Sci.*, 2000, **3**, 234–258.

2 R. Aucejo, J. Alarcón, C. Soriano, M. C. Guillem, E. García-España and F. J. Torres, *J. Mater. Chem.*, 2005, **15**, 2920–2927.

3 L. Fu, H. Zhang, S. Wang, Q. Meng, K. Yang and J. Ni, *J. Sol–Gel Sci. Technol.*, 1999, **15**, 49–55.

4 B. D. McCraith, C. McDonagh, A. K. Mcevoy, T. Butler, G. O'Keeffe and V. Murphy, *J. Sol–Gel Sci. Technol.*, 1997, **8**, 1053–1061.

5 F. Pina, J. C. Lima, C. Lodeiro, J. Seixas de Melo, P. Díaz, M. T. Albelda and E. García-España, *J. Phys. Chem. A*, 2002, **106**, 8207–8212.

6 M. T. Albelda, J. A. Aguilar, S. Alves, R. Aucejo, P. Díaz, C. Lodeiro, J. C. Lima, E. García-España, F. Pina and C. Soriano, *Helv. Chim. Acta*, 2003, **86**, 3118–3135.

7 M. T. Albelda, P. Díaz, E. García-España, J. C. Lima, C. Lodeiro, J. Seixas de Melo, A. J. Parola, F. Pina and C. Soriano, *Chem. Phys. Lett.*, 2002, **353**, 63–68.

8 E. García-España, M.-J. Ballester, F. Lloret, J.-M. Moratal, J. Faus and A. Bianchi, *J. Chem. Soc., Dalton Trans.*, 1988, **1**, 101–104.

9 M. Fontanelli and M. Micheloni, *Proceedings of the I Spanish - Italian Congress on Thermodynamics of Metal Complexes*, Diputación de Castellón, Castellón, Spain, 1990.

10 (*a*) G. Gran, *Analyst*, 1952, **77**, 661–671; (*b*) F. J. Rossetti and H. Rossetti, *J. Chem. Educ.*, 1965, **42**, 375–378.

11 (*a*) A. Sabatini, A. Vacca and P. Gans, *Coord. Chem. Rev.*, 1992, **120**, 389–405; (*b*) P. Gans, A. Sabatini and A. Vacca, *Talanta*, 1996, **43**, 1739–1753.

12 P. Gans, Program to determine the distribution of species in multiequilibria systems from the stability constants and mass balance equations, *Hyperquad Simulation and Speciation (HySS)*, Protonic Software, Leeds, England, 2006.

13 J. Jiao, S. Altrwasser, W. Wang, J. Weitkamp and M. Hunger, *J. Phys. Chem. B*, 2004, **108**, 14304–14310.

14 S. Ek, E. I. Iiskola, L. Niinistö, J. Vaittinen, T. T. Pakkanen and A. Root, *J. Phys. Chem. B*, 2004, **108**, 11454–11463.

15 A. P. de Silva, D. B. Fox, A. J. M. Huxley and T. S. Moody, *Coord. Chem. Rev.*, 2000, **205**, 41–57.

16 A. P. de Silva, H. Q. N. Gunaratne, T. Gunnlaugsson, A. J. M. Huxley, C. P. McCoy, J. T. Rademacher and T. E. Rice, *Chem. Rev.*, 1997, **97**, 1515–1566.

17 S. Alves, F. Pina, M. T. Albelda, E. García-España, C. Soriano and S. V. Luis, *Eur. J. Inorg. Chem.*, 2001, **2**, 405–412.

18 R. Aucejo, J. Alarcón, E. García-España, J. M. Llinares, K. L. Marchin, C. Soriano, C. Lodeiro, M. A. Bernardo, F. Pina, J. Pina and J. Seixas de Melo, *Eur. J. Inorg. Chem.*, 2005, **21**, 4301–4308.